Intracavity continuous-wave multiple stimulated-Raman-scattering emissions in a KTP crystal pumped by a Nd:YVO_4 laser

C. Y. Lee,[1] C. C. Chang,[1] C. L. Sung,[1] and Y. F. Chen[1,2,*]

[1]*Department of Electrophysics, National Chiao Tung University, Hsinchu, Taiwan*
[2] *Department of Electronics Engineering, National Chiao Tung University, Hsinchu, Taiwan*
[*]*yfchen@cc.nctu.edu.tw*

Abstract: Intracavity continuous-wave (CW) multiple stimulated-Raman-scattering emissions have been successfully demonstrated in a KTP crystal pumped by a Nd:YVO_4 1064-nm laser for the first time. Three different output couplers (OCs) with high-reflection (HR) coating in the range of 1-1.1, 1-1.13, and 1-1.15 μm are employed in the experiment to generate lasing wavelengths at 1095 (the first-Stokes emission of the 266 cm^{-1} Raman shift), 1095 + 1128 (the first- and second-Stokes emission of the 266 cm^{-1} Raman shift), and 1095 + 1128 + 1149 nm (the first two Stokes emissions of the 266 cm^{-1} Raman shift and the first-Stokes emission of the 694 cm^{-1} Raman shift), separately. This Raman laser paves a way to produce more-closely spaced set of CW emission in the green-yellow region.

OCIS codes: (140.3480) Lasers, diode-pumped; (140.3550) Lasers, Raman; (140.3580) Lasers, solid-state.

References and links

1. F. Weigl, "A generalized technique of two-wavelength, nondiffuse holographic interferometry," Appl. Opt. **10**(1), 187–192 (1971).
2. S. N. Son, J. J. Song, J. U. Kang, and C. S. Kim, "Simultaneous second harmonic generation of multiple wavelength laser outputs for medical sensing," Sensors **11**(6), 6125–6130 (2011).
3. P. Boixeda, L. P. Carmona, S. Vano-Galvan, P. Jaén, and S. W. Lanigan, "Advances in treatment of cutaneous and subcutaneous vascular anomalies by pulsed dual wavelength 595- and 1064-nm application," Med. Laser Appl. **23**(3), 121–126 (2008).
4. N. G. Basov, M. A. Gubin, V. V. Nikitin, A. V. Nikuchin, V. N. Petrovskii, E. D. Protsenko, and D. A. Tyurikov, "Highly-sensitive method of narrow spectral-line separations, based on the detection of frequency resonances of a 2-mode gas-laser with non-linear absorption," Izv. Akad. Nauk SSSR, Ser. Fiz. **46**, 1573–1583 (1982).
5. R. W. Farley and P. D. Dao, "Development of an intracavity-summed multiple-wavelength Nd:YAG laser for a rugged, solid-state sodium lidar system," Appl. Opt. **34**(21), 4269–4273 (1995).
6. Y. F. Chen, Y. S. Chen, and S. W. Tsai, "Diode-pumped Q-switched laser with intracavity sum frequency mixing in periodically poled KTP," Appl. Phys. B **79**(2), 207–210 (2004).
7. Y. J. Huang, Y. S. Tzeng, C. Y. Tang, S. Y. Chiang, H. C. Liang, and Y. F. Chen, "Efficient high-power terahertz beating in a dual-wavelength synchronously mode-locked laser with dual gain media," Opt. Lett. **39**(6), 1477–1480 (2014).
8. Y. J. Huang, Y. S. Tzeng, C. Y. Tang, and Y. F. Chen, "Efficient dual-wavelength synchronously mode-locked picosecond laser operating on the $^4F_{3/2}\rightarrow{}^4I_{11/2}$ transition with compactly combined dual gain media," IEEE J. Sel. Top. Quantum Electron. **39**(6), 1477–1480 (2014).
9. G. Q. Xie, D. Y. Tang, H. Luo, H. J. Zhang, H. H. Yu, J. Y. Wang, X. T. Tao, M. H. Jiang, and L. J. Qian, "Dual-wavelength synchronously mode-locked Nd:CNGG laser," Opt. Lett. **33**(16), 1872–1874 (2008).
10. G. Q. Xie, D. Y. Tang, W. D. Tan, H. Luo, S. Y. Guo, H. H. Yu, and H. J. Zhang, "Diode-pumped passively mode-locked Nd:CTGG disordered crystal laser," Appl. Phys. B **95**(4), 691–695 (2009).
11. H. Yoshioka, S. Nakamura, T. Ogawa, and S. Wada, "Dual-wavelength mode-locked Yb:YAG ceramic laser in single cavity," Opt. Express **18**(2), 1479–1486 (2010).
12. C. Y. Cho, P. H. Tuan, Y. T. Yu, K. F. Huang, and Y. F. Chen, "A cryogenically cooled Nd:YAG monolithic laser for efficient dual-wavelength operation at 1061 and 1064 nm," Laser Phys. Lett. **10**(4), 045806 (2013).

#244261 Received 2 Jul 2015; revised 6 Aug 2015; accepted 17 Aug 2015; published 20 Aug 2015

13. C. Y. Cho, T. L. Huang, S. M. Wen, Y. J. Huang, K. F. Huang, and Y. F. Chen, "Nd:YLF laser at cryogenic temperature with orthogonally polarized simultaneous emission at 1047 nm and 1053 nm," Opt. Express **22**(21), 25318–25323 (2014).
14. Y. T. Chang, Y. P. Huang, K. W. Su, and Y. F. Chen, "Diode-pumped multi-frequency Q-switched laser with intracavity cascade Raman emission," Opt. Express **16**(11), 8286–8291 (2008).
15. H. Zhu, Z. Shao, H. Wang, Y. Duan, J. Zhang, D. Tang, and A. A. Kaminskii, "Multi-order Stokes output based on intra-cavity $KTiOAsO_4$ Raman crystal," Opt. Express **22**(16), 19662–19667 (2014).
16. H. M. Pask, P. Dekker, R. P. Mildren, D. J. Spence, and J. A. Piper, "Wavelength-versatile visible and UV sources based on crystalline Raman lasers," Prog. Quantum Electron. **32**(3–4), 121–158 (2008).
17. H. J. Eichler, G. M. A. Gad, A. A. Kaminskii, and H. Rhee, "Raman crystal lasers in the visible and near-infrared," J. Zhejiang Univ. Sci. **4**(3), 241–253 (2003).
18. A. A. Kaminskii, K. Ueda, H. J. Eichler, Y. Kuwano, H. Kouta, S. N. Bagaev, T. H. Chyba, J. C. Barnes, G. M. A. Gad, T. Murai, and J. Lu, "Tetragonal vanadates YVO_4 and $GdVO_4$ – new efficient $\chi^{(3)}$-materials for Raman lasers," Opt. Commun. **194**(1–3), 201–206 (2001).
19. Y. F. Chen, "High-power diode-pumped actively Q-switched Nd:YVO_4 self-Raman laser: influence of dopant concentration," Opt. Lett. **29**(16), 1915–1917 (2004).
20. Y. F. Chen, "Efficient 1521-nm Nd:$GdVO_4$ Raman laser," Opt. Lett. **29**(22), 2632–2634 (2004).
21. J. Findeisen, H. J. Eichler, and P. Peuser, "Self-stimulating, transversally diode pumped Nd^{3+}:$KGd(WO_4)_2$ Raman laser," Opt. Commun. **181**(1–3), 129–133 (2000).
22. R. Lan, S. Ding, M. Wang, and J. Zhang, "A compact passively Q-switched $SrWO_4$ Raman laser with mode-locked modulation," Laser Phys. Lett. **10**(2), 025801 (2013).
23. Y. F. Chen, K. W. Su, H. J. Zhang, J. Y. Wang, and M. H. Jiang, "Efficient diode-pumped actively Q-switched Nd:YAG/$BaWO_4$ intracavity Raman laser," Opt. Lett. **30**(24), 3335–3337 (2005).
24. Z. Liu, Q. Wang, X. Zhang, Z. Liu, J. Chang, H. Wang, S. Zhang, S. Fan, W. Sun, G. Jin, X. Tao, S. Zhang, and H. Zhang, "A KTiOAsO4 Raman laser," Appl. Phys. B **94**(4), 585–588 (2009).
25. H. M. Pask, "The design and operation of solid-state Raman lasers," Prog. Quantum Electron. **27**(1), 3–56 (2003).
26. L. I. Ivleva, T. T. Basiev, I. S. Voronina, P. G. Zverev, V. V. Osiko, and N. M. Polozkov, "$SrWO_4$:Nd^{3+} – new material for multifunctional laser," Opt. Mater. **23**(1–2), 439–442 (2003).

1. Introduction

Lasers with simultaneous multi-wavelength emission are of scientific interest and have led to many potential applications, including holography, medical instrumentation, laser spectroscopy, LIDAR, and nonlinear optical mixers [1–6]. Recently, simultaneous multi-color emission have been successfully achieved by physically combining dual crystals as a composite gain medium [7,8] or directly employing a series of disordered crystals, which are characterized by multiple fluorescent peaks with comparable intensities, as the gain medium [9,10]. Another possible approach for the the multi-wavelength emission is exploiting laser crystals with a broad gain bandwidth, such as Ytterbium-doped media [11]. Based on the temperature-dependent fluorescence spectrum, the multi-wavelength operation can also be accomplished in Neodymium-doped lasers at cryogenic temperatures [12,13]. Moreover, nonlinear frequency conversions are widely used method to realize multi-wavelength emission [14–17].

Stimulated Raman scattering (SRS) is a well-known third-order nonlinear optical process to generate laser output in new spectral lines which are hard to reach directly for conventional solid-state lasers. A variety of crystals such as YVO_4 [18,19], $GdVO_4$ [20], $KGd(WO_4)_2$ [21], $SrWO_4$ [22], and $BaWO_4$ [23] are found to be promising candidates for efficient SRS. Recently, potassium titanyl phosphate (KTP) and its isomorph potassium titanyl arsenate (KTA) which are famous nonlinear optical crystals for second-order nonlinear optical processes have been experimentally demonstrated to be prominent Raman-active media [14,15]. Compared with the aforementioned Raman-active crystals, KTP and KTA crystals possess smaller primary Raman shift which is beneficial to generate multi-frequency radiation through cascade SRS [14,15]. Although the multi-wavelength emission created by the KTP-based intracavity cascade SRS have been developed in the Q-switched approach [14], the continuous-wave (CW) operation has not been demonstrated so far.

In this work, three different output couplers are exploited to realize the intracavity CW SRS wavelength conversions with the single and multiple Raman shifts in a KTP crystal pumped by a Nd:YVO_4 1064-nm laser for the first time. The first output coupler (OC1) with the high-reflection coating in the range of 1000-1100 nm is used to produce the first-Stokes

#244261 Received 2 Jul 2015; revised 6 Aug 2015; accepted 17 Aug 2015; published 20 Aug 2015

1095-nm emission of the Raman shift of 266 cm^{-1}. The output power can be up to 0.81 W at a pump power of 16.5 W. The second output coupler (OC2) with high reflectivity in the range of 1000-1130 nm is employed to simultaneously generate the first-Stokes 1095-nm and the second-Stokes 1128-nm emissions of the Raman shift of 266 cm^{-1}. The output powers of 0.15 W at 1095 nm and 0.68 W at 1128 nm can be obtained at a pump power of 16.5 W. The third output coupler (OC3) with the high reflectivity in a wider range of 1000-1500 nm is utilized to simultaneously generate the first two Stokes emissions of the Raman shift of 266 cm^{-1} and the first Stokes emission of the Raman shift of 694 cm^{-1}. At a pump power of 15 W, the generated output powers are 0.06 W at 1095 nm, 0.15 W at 1128 nm, and 0.35 W at 1149 nm. Experimental results reveal that it is feasible for generating multiple SRS emissions with a KTP crystal as the Raman-active medium in CW operation. We believe that the reflectivity of output coupler and the length of KTP crystal can be further optimized for power scaling.

2. Experimental setup

The experimental configuration was schematically depicted in Fig. 1. The laser resonator was composed of a front mirror, a gain medium, a Raman-active medium, and an output coupler. The gain medium was an *a*-cut 0.3 at.% Nd:YVO_4 crystal with a length of 8 mm and a transverse aperture of 3 × 3 mm^2 diffusion bonded with a 2.5-mm undoped YVO_4 crystal at the pump end. Both end facets of the composite crystal were antireflection (AR) coated at the fundamental wavelength of 1064 nm. The Raman-active medium was an *x*-cut ($\theta = 90°$ and $\phi = 0°$) 5 × 5 × 30 mm^3 KTP crystal with AR coating at 1064 nm on both end surfaces. The crystallographic *z* axis of the KTP crystal was oriented to be parallel to the *c* axis of the Nd:YVO_4 crystal due to the higher Raman gain coefficient compared to the X(YZ)X configuration as shown in Fig. 2. The spontaneous Raman spectrum was measured by a laser Raman spectrometer (Avantes, AvaRaman-532). Referring to Fig. 2, the primary and secondary Raman shifts can be found to locate at 266 and 694 cm^{-1}, respectively. The Raman gain coefficient for KTP crystal was approximately 2.5 cm/GW, which was similar to KTA crystal [24] but was slightly smaller than that for the other popular Raman media listed above (i.e. YVO_4, $GdVO_4$, $KGd(WO_4)_2$, $BaWO_4$, and $SrWO_4$) [18,25,26]. Both the YVO_4/Nd:YVO_4 composite crystal and KTP crystal were wrapped with indium foils and housed in water-cooled copper blocks to ensure laser working in stable operation. The water temperature was maintained at 16 °C.

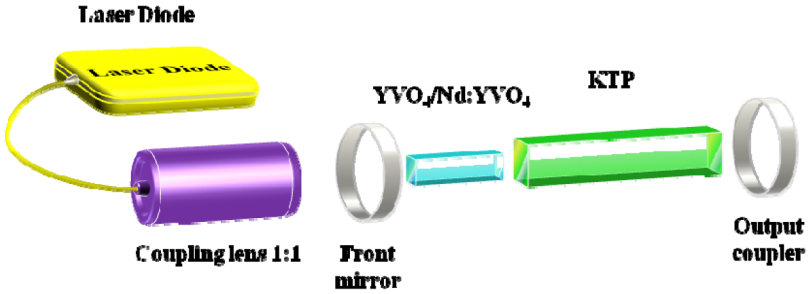

Fig. 1. Experimental configuration for an end-pumped YVO4/Nd:YVO4 laser with KTP crystal as an intra-cavity Raman crystal.

#244261 Received 2 Jul 2015; revised 6 Aug 2015; accepted 17 Aug 2015; published 20 Aug 2015

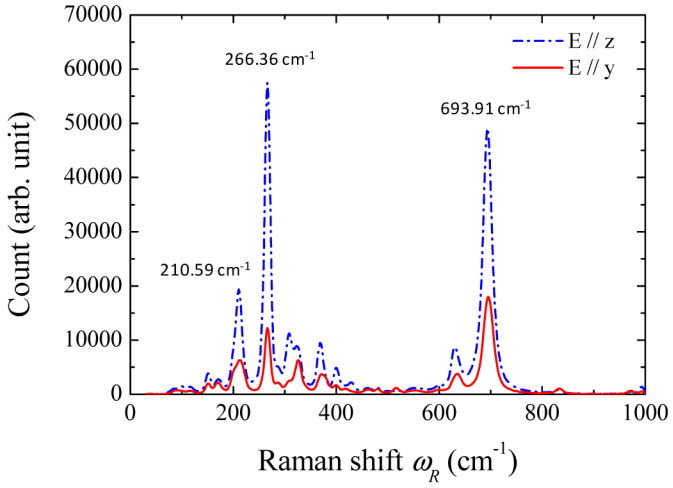

Fig. 2. The spontaneous Raman spectra of the KTP crystal in the X(ZZ)X and X(YZ)X configurations.

The pump source was a 20-W fiber-coupled 808-nm diode laser with a fiber core diameter of 200 μm and a numerical aperture of 0.22. A focusing lens set with 50-mm focal length and 85% coupling efficiency was used to reimage the pump beam into the laser crystal. The averaged pump spot size was approximately 100 μm. The front mirror was a 200-mm radius-of-curvature plano-concave mirror with AR coating at 808 nm on the entrance facet and with HR coating in the range of 1000-1200 nm (R > 99.5%) together with high-transmittance coating at 808 nm on the second facet. Three flat output couplers with different HR coated range as plotted in Fig. 3 were utilized to generate numerous CW SRS multi-wavelength emissions through the experiment. The reflection spectrum was measured by the monochromator (Jobin-Yvon, Triax 320). The reflectivities at wavelengths of 1064, 1095, 1128, and 1149 nm were 99.8%, 99.7%, 85.8% and 36.4% for OC1, and were 99.8%, 99.7%, 99.0%, and 54.6% for OC2, and were 99.8%, 99.7%, 99.6%, and 99.1% for OC3, respectively. All the optical components were arranged as compact as possible with a cavity length of 45 mm. With ABCD matrix, the cavity mode sizes for the fundamental and different Stokes waves were calculated to be around 150 μm.

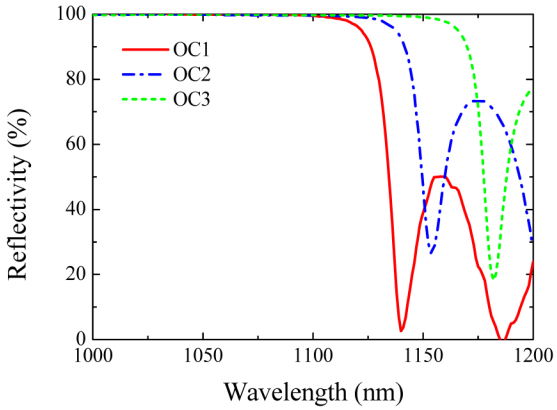

Fig. 3. The reflection spectra for the used output couplers.

#244261 Received 2 Jul 2015; revised 6 Aug 2015; accepted 17 Aug 2015; published 20 Aug 2015

3. Experimental results

To reach the high SRS threshold, it is important to utilize HR coated cavity mirrors for forming a high-Q Fabry-Perot cavity in CW Raman lasers. Therefore, three output couplers with different HR coated ranges were employed in our experiment. At first, we used OC1 with HR coating in the range from 1000 to 1100 nm to generate the first-Stokes emission line at 1095 nm, corresponding to the Raman shift of 266 cm^{-1}. The average output powers for the fundamental and first-Stokes emissions with respect to the incident pump powers are plotted in Fig. 4(a). The lasing thresholds were approximately 0.5 and 3.4 W for the fundamental and first-Stokes waves, respectively. As we can see that the fundamental average output power is clamped at a level of around 40 mW when the incident pump power beyond the threshold power of the first-Stokes wave. Once the pump power exceeded the SRS threshold of 3.4 W, the first-Stokes radiation began to emit and increased linearly with the pump power. At an incident pump power of 16.5 W, a maximum SRS output power of 0.81 W was obtained, which corresponds to the diode-to-Stokes conversion efficiency of approximately 5%. Figure 5(a) shows the optical spectrum of the laser output at the same pump power. The spectral information was monitored by an optical spectrum analyzer (Advantest, Q8347) which employs a Michelson interferometer with a resolution of 0.117 nm in the scanning region of 1000-1200 nm. Referring to Fig. 5(a), we can obviously find that no the second-Stokes wavelength at 1128 nm or the first-Stokes wavelength at 1149 nm, corresponding to the Raman shift of 694 cm^{-1}, is detected. It is the fact that the relatively lower reflectivities at these two wavelengths, compared to 1095 nm, cause a lower Q factor for the resonator and result in significantly higher SRS thresholds.

To obtain the second-Stokes emission line at 1128 nm, OC1 was replaced by OC2, which was HR coated from 1000 to 1130 nm with the reflectivity of 99.0% at 1128 nm. The average output powers for the fundamental and individual Stokes components versus the incident pump powers and the optical spectrum measured at an incident pump power of 16.5 W are displayed in Fig. 4(b) and 5(b), respectively. Owing to the increase of the reflectivity at 1128 nm, the second-Stokes wave of the 266 cm^{-1} Raman shift could be experimentally found when the pump power surpassed 9 W. The lasing thresholds for emission lines at 1064 and 1095 nm were almost the same as that of OC1 due to the same reflectivities. Different from the results of OC1, the output power for the first-Stokes field was suppressed and saturated at a level of around 0.15 W according to the appearance of the second-Stokes wave, as shown in Fig. 4(b). After the second-Stokes emission line at 1128 nm appeared, the SRS output power at this wavelength increased quickly with the pump power and eventually became the dominant portion of the Raman output, as shown in Fig. 5(b). The total SRS output power of 0.81 W, including the first- and second-Stokes waves of 0.67 and 0.14 W, was measured at the maximum pump power of 16.5 W.

Finally, in the case of utilizing OC3 with HR coating in the range of 1000-1150 nm, in addition to the Stokes wavelengths generated by the primary Raman shift of 266 cm^{-1}, the SRS emission line based the secondary Raman shift of 694 cm^{-1} could also be created. As depicted in Fig. 4(c), we could see that the lasing threshold for the wavelength at 1149 nm was approximately 11 W. The overall performances of the fundamental and Stokes waves for OC3 was similar to that of OC2 except the threshold power at 1128 nm was decreased to approximately 5 W due to a higher reflectivity of 99.6% at this wavelength. When the incident pump power exceeded 15.1 W, the thermal induced roll-over phenomenon for KTP crystal was experimentally observed because of the additional generation of the first-Stokes wave at 1149 nm. Therefore, the maximum pump power for OC3 was limited to be 15.1 W. At the pump power of 15.1 W, a total SRS output power of 0.56 W was obtained, containing the first- and second-Stokes components of 0.06 and 0.15 W for the primary Raman shift and the first-Stokes component of 0.35 W for the secondary Raman shift. Figure 5(c) displays the optical spectrum for OC3 under the pump power of 15.1 W. Once again, we can find that the emission line at 1149 nm eventually becomes the dominant portion of the laser output. With the experimental results represented here, various CW multi-wavelength emissions have been

#244261 Received 2 Jul 2015; revised 6 Aug 2015; accepted 17 Aug 2015; published 20 Aug 2015

successfully achieved by the intracavity SRS wavelength conversion with the single and multiple Raman shift in a KTP crystal.

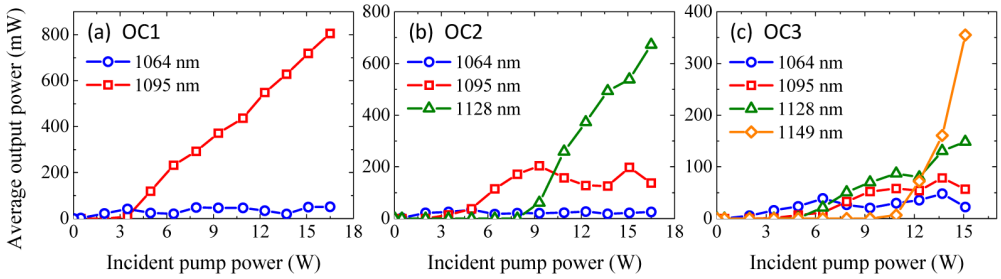

Fig. 4. Average output powers of the Stokes waves and the fundamental wave with respect to incident pump powers for different output couplers.

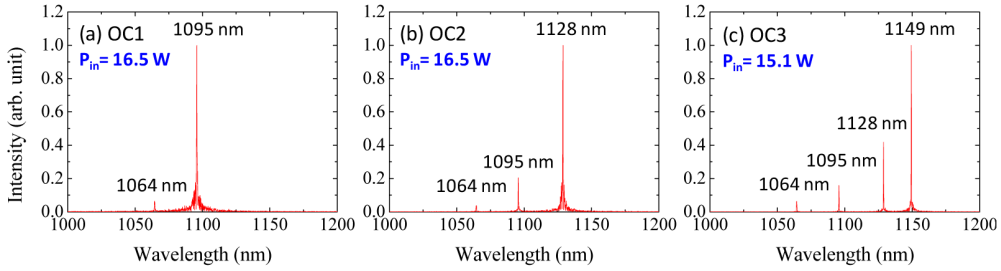

Fig. 5. Lasing spectra for (a) OC1 at incident pump power of 16.5 W, (b) OC2 at incident pump power of 16.5 W, and (c) OC3 at incident pump power of 15.1 W.

4. Conclusion

In summary, we utilize three output couplers to realize for the first time to our knowledge the intracavity CW SRS multiple emissions with the single and multiple Raman shift in a KTP crystal pumped by a Nd:YVO_4 1064-nm laser. The OC1 with HR coating in the range of 1000-1100 nm is employed to produce the first-Stokes 1095-nm emission of the Raman shift of 266 cm^{-1}. The OC2 with HR coating in the range of 1000-1130 nm is applied to simultaneously generate the first-Stokes 1095-nm and the second-Stokes 1128-nm emissions of the 266 cm^{-1} Raman shift. Finally, the OC3 with the high reflectivity in a wider range of 1000-1150 nm is exploited to simultaneously generate the first two Stokes emissions of the 266 cm^{-1} and the first-Stokes 1149-nm emission of the Raman shift of 694 cm^{-1}. These experimental results shown here pave a way to create more-closely spaced set of CW emission in the green-yellow region.

Acknowledgments

The authors thank the National Science Council for the financial support of this research under Contract No. MOST 103-2112-M-009-0016-MY3.

#244261 Received 2 Jul 2015; revised 6 Aug 2015; accepted 17 Aug 2015; published 20 Aug 2015